Journal of Optoelectronics and Advanced Materials Vol. 5, No. 3, September 2003, p. 615 - 620

FLUX GROWTH, MORPHOLOGY AND COMPOSITION OF $YAl_3(BO_3)_4$ CRYSTALS DOPED WITH Pr, Ho, Yb, Tm

E. V. Koporulina*, O. V. Pilipenko, V. V. Maltsev, N. I. Leonyuk, A. V. Mokhov[a]

Moscow State University, Geological Faculty, Moscow 119992/GSP-2, Russian Federation
[a]Institute of Ore Deposits Geology, Petrography, Mineralogy and Geochemistry, Moscow 119017, Russian Federation

This paper reports new data on flux growth and characterization of $(R,Y)Al_3(BO_3)_4$ (R = Pr, Ho, Yb, Tm) single crystals obtained using potassium trimolybdate and lead fluoride based systems. The average R distribution coefficients were found to be 0.53 to 1.02 for different rare earth elements. Two morphological types of $(Tm,Y)Al_3(BO_3)_4$ crystals were characterized. The visible luminescence spectra of $(Pr,Y)Al_3(BO_3)_4$ and $PrAl_3(BO_3)_4$ at 10 K and room temperature were measured.

(Received July 10, 2003; accepted July 31, 2003)

Keywords: Rare earth aluminium borates, Solid solutions, Flux crystallization, Crystal morphology

1. Introduction

Borate crystals with a general formula $RAl_3(BO_3)_4$ (RAB) (R=Y, La-Lu) can be considered as polyfunctional materials having device potential due to their good thermal and chemical stability and a possibility of wide isomorphous substitutions. Most of them belong to the huntite type of structure with *R*32 space group (low-RAB) [1], but Nd-, Gd-, Sm-, Eu- and Pr-representatives also have high temperature monoclinic modifications (high-RAB) with the phase transitions at 880-900 ^oC, 1040-1050 ^oC, 1130-1150 ^oC, 1130-1150 ^oC and 1080 ^oC respectively [2-4]. Of this borate family, the non-centrosymmetric $R_xY_{1-x}Al_3(BO_3)_4$ (RYAB) crystals with R = Nd^{3+}, Er^{3+}, Yb^{3+} are of highest interest as promising solids for lasing and non-linear optical applications [5-8]. Optical and acoustic characteristics of these borates with R = Gd^{3+} and Eu^{3+} have been reported in Ref. [9-11]. The Pr^{3+} doped crystals have a potential as laser materials in the UV region. The optical spectra of PYAB and PAB have also been studied [12,13]. Among a number of publications on crystal growth and characterization of these compounds (see, for example, Refs. [14-19]), there are no systematic investigations of composition, homogeneity, morphology and structural characteristics of above solid solutions depending on the flux growth conditions. In the present work, we consider the system $(R,Y)Al_3(BO_3)_4$, where R = Pr, Ho, Yb and Tm. The visible luminescence spectra of PYAB and PAB at 10 K and room temperature have been measured in order to obtain further information about the concentration dependence of the Pr^{3+} emission properties in these materials.

2. Experimental details

The crystals $R_xY_{1-x}Al_3(BO_3)_4$, x = 0.1, 0.05, 0.03 (R = Ho), x = 0.11, 0.09, 0.07, 0.05, 0.025, 0.005 (R = Tm), and x = 0.05, 0.025, 0.005 (R = Yb) were prepared by spontaneous nucleation using

* Corresponding author: evkop@geol.msu.ru

$K_2Mo_3O_{10}$ based fluxes in the temperature range of 1120-900 °C. Rare earth doped YAB crystalline substances in the starting solutions were 20 wt% and 17 wt.%. According to the Ref. [4], the field of $YAl_3(BO_3)_4$ (YAB) primary crystallization in the system YAB-($K_2Mo_3O_{10}$-B_2O_3-Y_2O_3) has wider temperature-concentration boundaries at 17 wt% in comparison with 20 wt.%. Consequently, this flux composition is more convenient for growth of slightly doped YAB crystals. As it was shown earlier [4], PbF_2 based fluxes are more preferable for PrAl-borate. Hence, the complex flux PbF_2-B_2O_3 was used for $(Pr_xY_{1-x})Al_3(BO_3)_4$ (PYAB), x = 0.05, 0.025, 0.005 crystallization. Starting chemicals in all runs were Y_2O_3, R_2O_3 (R = Pr, Ho, Tm, Yb), PbF_2, Al_2O_3 and B_2O_3, but $K_2Mo_3O_{10}$ was previously synthesized from K_2MoO_4 and H_2MoO_4 at 650 °C.

Platinum crucibles with the initial mixture were kept at 1050-1120°C for 1-4 hours and cooled down to 900 °C at a rate of 0.2-0.5 °C/h (4.8-12 °C/day). Then, the temperature was lowered to 350 °C at the rate of 10 °C/h.

The composition, homogeneity and external morphology of grown crystals were studied by the analytical scanning electron microscope (ASEM) JSM-5300 + Link ISIS. Microprobe analysis of polishing samples was performed with an accuracy of 0.2-0.3 wt %. A Cameca analyzer was used for the study of the crystal with minor dopant concentration. In this case the accuracy has been increased up to 0.02-0.03 wt.%. The X-ray powder diffraction pattern of solids were obtained using INEL and DRON-1UM diffractometers.

The distribution coefficients (*K*) of Pr, Tm, Ho and Yb were calculated on the basis of the equation $K=C_{cryst}/C_{diss.RYAB}$, where C_{cryst} is R content in RYAB grown crystals and $C_{diss.RYAB}$ is R concentrations in the borate crystalline substances of the melt.

3. Results and discussion

The typical size of the crystals grown was up to 2 × 2 × 5 mm^3. (Yb,Y)Al- and (Tm,Y)Al-borate crystals are colorless, but (Pr,Y)Al- and (Ho,Y)Al-samples have light green and light pink color respectively. Crystals $(Yb,Y)Al_3(BO_3)_4$ and $(Ho,Y)Al_3(BO_3)_4$ have the well known set of simple crystallographic forms of the borate family: two trigonal prisms $\{11\bar{2}0\}$, $\{2\bar{1}\bar{1}0\}$ and rombohedron $\{10\bar{1}1\}$.

Among $Tm_xY_{1-x}Al_3(BO_3)_4$ (TYAB) borates, two morphologically different types of the crystals are distinguished. First type shows elongated crystals along third axis (elongation 4-6.5) (Fig 1a).

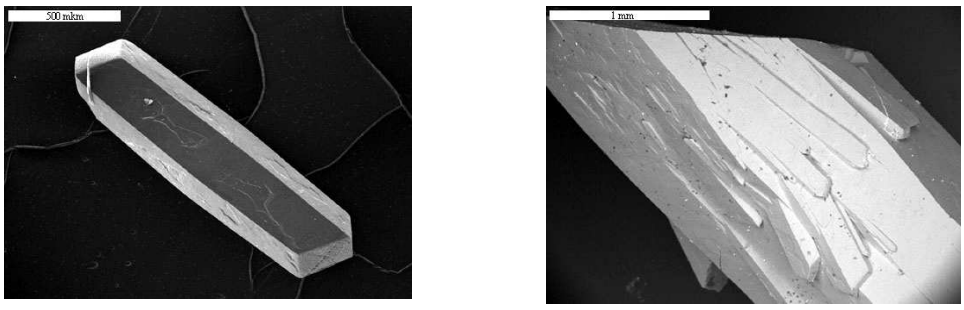

a b

Fig. 1. Habit (a) and micromorphology (b) of first type of TYAB crystals.

SEM photographs show splitting strongly developed on the trigonal prism faces (Fig. 1b). Rombohedron faces of these crystals consist of separate disordered blocks (Fig. 2a,b) and no smooth areas are found on these $\{10\bar{1}1\}$ faces. «Steps», formed due to this splitting, are related to the crystal type and frequently propagate from a prism face to rombohedron (Fig. 2b). X-ray pattern of the mixed split crystals does not differ from those for YAB with huntite structure (Table 1). The second type of TYAB crystals shows smooth prism and rombohedron faces and their elongation is 2-2.5.

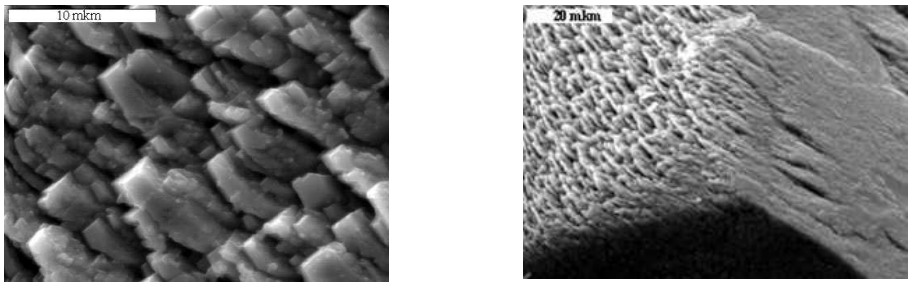

a b

Fig. 2. Micromorphology of rombohedron faces of first type TYAB crystals.

Table 1. X-ray powder diffraction data for the TYAB crystal (x=0.05).

Data of this work		$YAl_3(BO_3)_4$ [JSPDS # 15-117]	
d (Å)	I(%)	d (Å)	I(%)
5.42	28	5.34	60
4.68	3	4.63	40
3.53	11	3.50	60
3.31	7	3.29	40
2.81	9	2.80	40
2.69	100	2.69	100
2.33	9	2.32	80
2.15	8	2.14	60
2.136	5	2.128	60
1.939	3	1.937	40
1.901	10	1.898	40
1.796	9	1.792	40
1.766	2	1.765	30
1.757	2	1.754	40
1.675	6	1.673	60
1.654	4	1.651	40
1.470	2	1.470	30
1.419	3	1.420	40

Most PYAB crystals, grown in our experiments, also display growth striations on the trigonal prism faces (Fig. 3a). These growth striations are characteristic feature of high-temperature rare-earth aluminium borates. Any crystal of low modification series placed into supersaturated fluxed melts at the temperature higher than its phase transition point, exhibits growth striations which are specific for high monoclinic RAB [4].

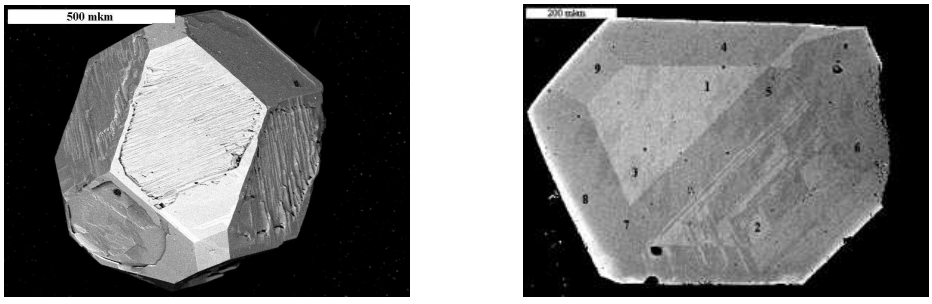

a b

Fig. 3. Typical morphology (a) and composition image (b) of PYAB crystals.

Table 2. Microprobe analyses of the $(Pr_xY_{1-x})Al_3(BO_3)_4$ crystal (x = 0.05).

Point number	PYAB crystal composition	K_{Pr}
1	$(Pr_{0.06}Y_{0.94})Al_3(BO_3)_4$	1.29
2	$(Pr_{0.05}Y_{0.95})Al_3(BO_3)_4$	0.91
3	$(Pr_{0.08}Y_{0.92})Al_3(BO_3)_4$	1.67
4	$(Pr_{0.02}Y_{0.98})Al_3(BO_3)_4$	0.37
5	$(Pr_{0.01}Y_{0.99})Al_3(BO_3)_4$	0.24
6	$(Pr_{0.01}Y_{0.99})Al_3(BO_3)_4$	0.12
7	$(Pr_{0.03}Y_{0.97})Al_3(BO_3)_4$	0.68
8	$(Pr_{0.03}Y_{0.97})Al_3(BO_3)_4$	0.54
9	$(Pr_{0.02}Y_{0.984})Al_3(BO_3)_4$	0.49

According to ASEM data, these crystals are very inhomogeneous. The backscattering electron image of these crystals is shown in Fig. 3b. Depending on the average atomic number the light grey areas contain much more amount of praseodymium in comparison with the dark grey ones (Table 2). X-ray patterns of these crystals correspond to the *R*32 space group (Table 3), but they are characterized by high background. This fact may be attributed to disordering in the crystal structure. For the first time, this type of disordering was discovered in $(Nd,Y)Al_3(BO_3)_4$ and $(Gd,Y)Al_3(BO_3)_4$ solid solutions [20]. In our case, the end members show high temperature monoclinic modifications. Therefore, it may be concluded, that specific morphology and composition of PYAB crystals are also connected with phase transition in their crystallization process.

Table 3. X-ray powder diffraction data for the PYAB crystal (x=0.05).

Data of this work		$YAl_3(BO_3)_4$ [JSPDS # 15-117]	
d (Å)	I(%)	d (Å)	I(%)
5.38	32	5.34	60
4.64	17	4.63	40
3.51	39	3.50	60
3.29	10	3.29	40
2.80	25	2.80	40
2.69	100	2.69	100
2.32	36	2.32	80
2.13	10	2.14	60
2.131	24	2.128	60
1.937	10	1.937	40
1.898	25	1.898	40
1.793	8	1.792	40
1.764	3	1.765	30
1.755	14	1.754	40
1.672	19	1.673	60
1.648	14	1.651	40
1.469	6	1.470	30
1.417	12	1.418	30
1.404	4	1.406	30
1.401	4	1.402	40
1.361	2	1.363	10
1.344	4	1.340	30

It was found that the average R distribution coefficients vary from 0.53-76 in PYAB to 1.02 in YbYAB crystals (Table 4). A main reason for the variation of the distribution coefficient is a difference in Y^{3+} and R^{3+} cation sizes. In the case of PYAB, when the Pr^{3+} cation radius is considerably higher that of than Y^{3+}, and it can be supposed that yttrium sites in $YAl_3(BO_3)_4$ (YAB) huntite structures are not ideally suitable for praseodymium. In contrast, the distribution coefficients of Ho, Yb and Tm are close to one as a consequence of minor difference in the sizes of Y^{3+} and R^{3+} cations. Relatively lower values of Tm^{3+} distribution coefficients for x = 0.7-0.11, are due most likely, to higher cooling rates of the melts during spontaneous crystallization.

The main band system of the room temperature spectra of the PYAB crystals is due to the $^1D_2 \rightarrow {}^3H_4$ transition and consists of at least seven components arising from the Stark structure of the involved levels. Its maximum lies at 605 nm. This is usually the main emission band present in the luminescence spectra of diluted Pr^{3+} doped materials. The weaker features observed at 645 and 649 nm are assigned to the $^3P_0 \rightarrow {}^3F_2$ transition. The other bands due to emissions from the $^3P_0$ level to lower states are very weak. It is interesting to note that when the Pr^{3+} concentration increases, the intensity of the $^1D_2 \rightarrow {}^3H_4$ band system decreases, indicating that the concentration quenching of the $^1D_2$ is present even at the relatively low Pr^{3+} doping levels of our samples. This concentration quenching has been attributed to energy migration and cross relaxation mechanisms (see, for example, the paper of R. C. Naik et al. [21] on YPO_4:Pr^{3+}). In the emission spectra PAB at the 298 K and the 10 K the $^1D_2 \rightarrow {}^3H_4$ band is weaker than the $^3P_0 \rightarrow {}^3F_2$ one, as a consequence of the concentration quenching of the emitting level. Moreover, it is evident the stronger temperature dependence of the emission from the $^1D_2$ level with respect to that from the $^3P_0$ one.

Table 4. Microprobe analysis of RYAB crystals.

RYAB composition in the fluxed melt	The average RYAB crystals composition	The average RE distribution coefficient (*K*)
$(\mathbf{Ho}_{0.01}Y_{0.99})Al_3(BO_3)_4$	$(Ho_{0.01}Y_{0.99})Al_3(BO_3)_4$	1.00
$(\mathbf{Ho}_{0.03}Y_{0.97})Al_3(BO_3)_4$	$(Ho_{0.03}Y_{0.97})Al_3(BO_3)_4$	1.00
$(\mathbf{Ho}_{0.05}Y_{0.95})Al_3(BO_3)_4$	$(Ho_{0.05}Y_{0.949})Al_3(BO_3)_4$	1.00
$(\mathbf{Yb}_{0.005}Y_{0.995})Al_3(BO_3)_4$	$(Yb_{0.005}Y_{0.953})Al_3(BO_3)_4$	1.00
$(\mathbf{Yb}_{0.025}Y_{0.975})Al_3(BO_3)_4$	$(Yb_{0.026}Y_{0.974})Al_3(BO_3)_4$	1.02
$(\mathbf{Yb}_{0.075}Y_{0.925})Al_3(BO_3)_4$	$(Yb_{0.075}Y_{0.925})Al_3(BO_3)_4$	1.00
$(\mathbf{Yb}_{0.05}Y_{0.95})Al_3(BO_3)_4$	$(Yb_{0.046}Y_{0.954})Al_3(BO_3)_4$	0.98
$(\mathbf{Pr}_{0.005}Y_{0.995})Al_3(BO_3)_4$	$(Pr_{0.003}Y_{0.997})Al_3(BO_3)_4$	0.60
$(\mathbf{Pr}_{0.025}Y_{0.975})Al_3(BO_3)_4$	$(Pr_{0.013}Y_{0.987})Al_3(BO_3)_4$	0.53
$(\mathbf{Pr}_{0.05}Y_{0.95})Al_3(BO_3)_4$	$(Pr_{0.038}Y_{0.952})Al_3(BO_3)_4$	0.76
$(\mathbf{Tm}_{0.005}Y_{0.995})Al_3(BO_3)_4$	$(Tm_{0.005}Y_{0.995})Al_3(BO_3)_4$	1.00
$(\mathbf{Tm}_{0.025}Y_{0.975})Al_3(BO_3)_4$	$(Tm_{0.024}Y_{0.976})Al_3(BO_3)_4$	0.98
$(\mathbf{Tm}_{0.05}Y_{0.95})Al_3(BO_3)_4$	$(Tm_{0.05}Y_{0.95})Al_3(BO_3)_4$	1.00
$(\mathbf{Tm}_{0.07}Y_{0.93})Al_3(BO_3)_4$	$(Tm_{0.06}Y_{0.95})Al_3(BO_3)_4$	0.80
$(\mathbf{Tm}_{0.09}Y_{0.91})Al_3(BO_3)_4$	$(Tm_{0.08}Y_{0.92})Al_3(BO_3)_4$	0.87
$(\mathbf{Tm}_{0.11}Y_{0.89})Al_3(BO_3)_4$	$(Tm_{0.09}Y_{0.91})Al_3(BO_3)_4$	0.84

Acknowledgements

The research described in this publication was supported, in part, by grants of Russian President for young scientists № MK-229.2003.05 and MK-1430.2003.05. The authors thank A. I. Tsepin and N. N. Kononkova for the electron microscopy investigations, E. Cavalli for optical measurements of grown crystals.

References

[1] A. D. Mills, Inorgan.Chem. **1**, 960 (1962).
[2] E. L. Belokoneva, M. A. Simonov, A. V. Pashkova, T. I. Timchenko, N. V. Belov. Doklady Akad.Nauk SSSR **25,** 948 (1980).
[3] E. L. Belokoneva, A. V. Pashkova, T. I. Timchenko, N. V. Belov, Doklady Akad. Nauk SSSR **26**, 1019, (1981).
[4] N. I. Leonyuk, L. I. Leonyuk, Prog.Crystal Growth and Charact. **31**, 179 (1995).
[5] N. I. Leonyuk, Prog.Crystal Growth and Charact. **31**, 279 (1995).
[6] H. Jiang, J. Li, X. Hu, H. Liu, B. Teng, Ch.-Q.Zhang, P.Dekker, P.Wang. J. Crystal Growth **233**, 248 (2001).
[7] X. Hu, J. Wang, J. Wei, Y. Liu, R. Song, M. Jiang. Prog. Crystal Growth and Charact. **40**, 57 (2000).
[8] D. A. Keszler, A. Akella, K. I. Schaffers, T. Alekel. Mat. Res.Soc.Symp.Proc. **329**, 15 (1994).
[9] F. Kellendonk, G. Blasse, J. Chem. Phys. **75**, 561 (1981).
[10] C. Gorller-Warland, E. Huygen, K. Binnemans, L. Fluyt, J. Phys. Condens. Matter **6**, 7796 (1994).
[11] G. Blasse, H. S. Kiliaan, A. J. de Vries, J. Luminescence **40-41**, 639 (1988).
[12] E. V. Koporulina, N. I. Leonyuk, D. Hansen, K. L. Bray, J. Cryst. Growth **191**, 767 (1998).
[13] Yu. V. Malyukin, P. N. Zhmurin, R. S. Borisov, M. Roth, N. I. Leonyuk. Opt. Commun. **201**, 355 (2002)
[14] N. I. Leonyuk, A. V. Pashkova, N. V. Belov, Kristall und Technik **14**, 47 (1979).
[15] V. Nikolov, P. Peshev, J. Crystal Growth **144**, 187 (1994).
[16] S. T. Jung, D. Y. Choi, J. K. Kang, S. J. Chung, J. Crystal Growth **148**, 207 (1995).
[17] X. B. Hu, S. S. Jiang, X. R. Huang, W. J. Liu, C. Z. Ge, J. Y. Wang, H. F. Pan, J. H. Jiang, Z. G. Wang J. Crystals Growth **173**, 460 (1997).
[18] G. Wang, H. G. Gallagher, T. P. J. Han, B. Henderson. J. Crystal Growth **163**, 272 (1996).
[19] E. L. Belokoneva, T. I. Timchenko. Kristallografiya **28**, 1118 (1983) (in Russian).
[20] E. V. Koporulina, N. I. Leonyuk, A. V. Mokohov, O. V. Pilipenko, G. Bocelli, L. Righi, J. Crystal Growth **211** 491-496 (2000)
[21] R. C. Naik, N. P. Karanjikar, M. A. N. Razvi, J. Lumin. **54**, 139, (1992).